ELSEVIER

Polymer 43 (2002) 7155–7160

polymer

www.elsevier.com/locate/polymer

# Bulk morphology and micellization of poly(diene)–poly(ethylene oxide) diblock copolymers in water

Y. Deng[a], R.N. Young[a,*], A.J. Ryan[a], J.P.A. Fairclough[a], A.I. Norman[a], R.D. Tack[b]

[a]*Department of Chemistry, Dainton Building, University of Sheffield, Sheffield S3 7HF, UK*
[b]*Infineum UK Limited, P.O. Box 1, Milton Hill, Abingdon, Oxfordshire OX13 6BB, UK*

Received 15 January 2002; received in revised form 20 March 2002; accepted 21 May 2002

**Abstract**

The morphologies of a range of poly(ethylene oxide) diblock copolymers with polybutadiene (PB–PEO) and with polyisoprene (PI–PEO) were determined by small-angle X-ray scattering (SAXS) and some comparative studies were made by rheology. These materials form micelles in water and the solutions give remarkably sharp SAXS patterns in which up to the sixth order reflection can be seen. The morphologies of two PEO diblocks formed from a commercial hydrogenated, mixed-architecture, polybutadiene (Kraton L1203®) have also been determined. Preliminary results are reported for a triblock copolymer poly(ethylene-*alt*-propylene)–polyethylene–PEO which has two crystallizable blocks. © 2002 Elsevier Science Ltd. All rights reserved.

*Keywords:* Amphiphilic; Diblock; Morphology

## 1. Introduction

Diblock copolymers of sufficiently high molecular weight microphase-separate in the melt state. The structure formed is strongly influenced by the volume fraction of each block and by the segment–segment interaction parameter $\chi$. In addition, the architecture [1], conformational asymmetry [2] and composition fluctuations [3] all have an effect. In the region of near equal volume fractions a lamellar phase is formed. As the composition moves away from equal volume fractions, first the hexagonal and then the Ia3d gyroid phases become more stable; finally, at the extremes of composition a bcc structure is preferred.

Amphiphilic block copolymers, which contain both hydrophilic and hydrophobic segments, are well known to form micelles in aqueous media. Such copolymers have a wide variety of applications as polysoaps, polymeric surfactants, solution modifiers, emulsifiers, wetting agents, foam stabilizers and drug carriers [4–7]. Large scale commercial material generally employs poly(ethylene oxide) (PEO) as the hydrophilic component and poly (propylene oxide) as the hydrophobic one [8]. Although poly(propylene oxide) is rather weakly hydrophobic at near-ambient temperatures, it is favoured on the grounds of cost.

A variety of studies has been made of copolymers of PEO attached to the strongly hydrophobic block polystyrene [9–12]. However, the high glass transition temperature of polystyrene makes it very difficult to disperse such diblocks in water or to achieve a state of equilibrium and, in this regard, blocks of PEO with the polydienes are much more amenable to study. Syntheses have been described involving polybutadiene [13–18] and polyisoprene [19–23]. Polydienes bearing a terminal hydroxyl functionality have been saturated by hydrogenation and then used to create a diblock with PEO [24,25].

The anionic polymerizations of ethylene oxide (EO), butadiene and isoprene are termination-free with appropriate organometallic initiators and yield products having low polydispersities and predictable molecular weights.

However, the direct creation of an AB diblock copolymer by successive polymerization of monomers A and B is only possible if they are supplied in the order of increasing electrophilicity. This requires the polymerization of EO to be initiated by a living polydiene block. The polymerization of EO proceeds smoothly with organopotassium reagents [26]; such initiators give rise to block copolymers in which the dienes are predominantly enchained in a 1,2- or 3,4-sense [19,21].

The microstructure obtained on anionically polymerizing

---

* Corresponding author. Tel.: +44-114-222-9418; fax: +44-114-273-8673.
*E-mail address:* r.young@sheffield.ac.uk (R.N. Young).

PII: S0032-3861(02)00457-3

isoprene or butadiene depends critically upon the choice of solvent and counterion [27]. If enchainment in the elastomeric 1,4-sense is desired, the polymerization of the diene can only be initiated by the combination of an organolithium initiator with a hydrocarbon solvent because the use of organometallics derived from other alkali metals or the use of polar solvents produce polydienes with high vinyl microstructures. Unfortunately, although organolithium initiators quantitatively add a single molecule of EO propagation does not ensue [28] unless a very potent complexing agent such as the phosphazene base $P_4$ *t*-butyl is also present [29,30]. It seems that the reactivity induced by this base is attributable to the complexation and dissociation of very strongly bonded unreactive aggregates formed by the alkoxy-lithium ion pairs. However, whereas such a protocol enables the preparation of diblock copolymers with polydienes having a high vinyl content by sequential polymerization, the synthesis of their counterparts having high 1,4-enchainment requires an indirect approach. One expedient route is to couple hydroxyl-terminated polydiene and polyethylene oxide homopolymers with a diisocyanate [13]. An alternative path adopted in the present work entails hydroxyethylation of polydienyl lithium followed by conversion to the ethoxy potassium salt to enable the formation of the PEO block—as outlined in Scheme 1 [31,32].

## 2. Experimental

Solvents, monomers and *sec*-butyl lithium were purified as described by Allgaier et al. [32]. The potassium salt of the dimer dianion of α-methyl styrene (KMS) was prepared under vacuum in a flask by contacting a solution of the monomer in THF with potassium metal in a side-arm attached via a glass frit. A greaseless stopcock on the flask enabled its attachment to other vessels and permitted the deep red solution to be dispensed.

### 2.1. Polymer synthesis

Living polydienes were prepared in benzene under high vacuum using *sec*-BuLi as initiator. An excess of EO ($EO/Li > 40$) was introduced and the reaction mixture was allowed to stand for an hour. The solution was neutralized with HCl then extracted with water to remove LiCl. The polymer was recovered, dried and dissolved in THF. The polymer hydroxyl end-groups were titrated with KMS solution; the approach of the end-point was indicated by the slowing discharge of the red colour of the added KMS. EO was introduced and the polymerization was allowed to proceed at 45 °C for 48 h, whereafter the reaction was terminated with acidified methanol. The polymer was recovered, dissolved in chloroform and washed with water to remove potassium salts and any homo-PEO that might be present.

Some of the hydroxyl terminated polydienes were converted to the corresponding functionalized polyolefins by hydrogenation with $H_2$ in cyclohexane using $Pd/CaCO_3$ as catalyst [33]. $^1$H NMR and GPC showed that the reduction was complete and that neither degradation nor cross-linking had occurred. These polymers, together with a sample of Shell Kraton L1203® (a hydroxyl terminated ethylene–butylene copolymer MW approximately 4200) were converted to EO block copolymers via their potassium salts. Because hydrogenated 1,4-PB is partly crystalline it was necessary to conduct its titration and the subsequent polymerization of the EO block at 50–60 °C to maintain a homogeneous solution.

### 2.2. Characterization

GPC was carried out using three 60 cm Polymer Laboratories 5 μm mixed gel columns. In all experiments the flow rate was 1 ml min$^{-1}$ and the eluant was THF/dimethyl acetamide (THF/DMA 90:10 v/v). $^1$H-NMR spectra were recorded using a Bruker AM-250 spectrometer with $CDCl_3$ as solvent. Small-angle X-ray scattering (SAXS) measurements were made on beamline 8.2 of the SRS at the CCLRC Laboratory, Daresbury, UK and the DUBBLE beamline at the European Synchrotron Radiation Facility (ESRF), Grenoble, France. Details of the equipment and methodology have been reported elsewhere [34,35].

SAXS patterns for the bulk copolymers were generated at 6 s intervals while the samples were heated at 10 °C min$^{-1}$ in a Linkam single pan DSC. Various temperature profiles and final temperatures were employed, conditional on the beamline and the sample. Data are presented as intensity vs. scattering vector, $q = (4\pi/\lambda)\sin\theta$, where $\lambda$ is the wavelength and $2\theta$ the scattering angle. The data was collected by a multiwire detector and normalized by the standard methods. For the SAXS characterization of the aqueous gels, the samples were loaded into the Linkam DSC at the SRS or into a hand shear cell at the ESRF. Samples were manually sheared by $\sim 300\%$ and at 1 Hz for 20 s to align them before placing them in the beam. No heating was applied, hence all the two-dimensional patterns were obtained at room temperature.

Rheological measurements were made using a Rheometrics RDA II instrument with 25 mm parallel plate geometry. Samples were heated under nitrogen until softened and pressed to a thickness of between 1.5 and 2.5 mm; after cooling, excess polymer was trimmed off. Dynamic strain measurements were made to determine the linear regime within which subsequent measurements were made.

## 3. Results and discussion

Scheme 1 summarises the route followed for the

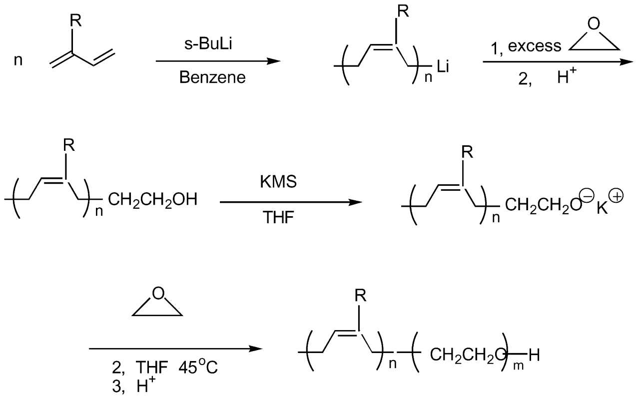

Scheme 1.

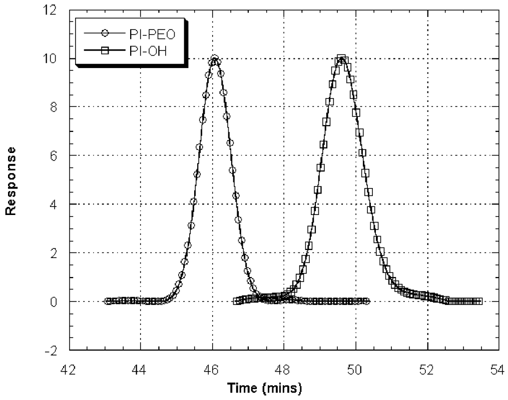

Fig. 1. GPC curves for PI–PEO diblock copolymer YD 45.

synthesis of the copolymers. Living polydiene was reacted with EO to create a terminal –OLi functionality. Conversion to –OH with hydrochloric acid and the removal of lithium salts was followed by titration to form the –OK terminated macroinitiator which was then employed to polymerize EO. Previous authors [20,24] have used solutions of potassium naphthalene or cumyl potassium as titrants but we found KMS to be more stable on storage than potassium naphthalene and more convenient than cumyl potassium since cumyl methyl ether—the precursor for the latter—is prone to decompose into α-methyl styrene and methanol which will form potassium methoxide, thereby, leading to contamination of the diblock by homo-PEO. Titration need not be continued to the end-point since rapid exchange between terminal –OH and –OK occurs. Experiments showed that failure to remove the lithium chloride from the PB–OH and PI–OH before titration led to bimodality in the GPC traces of the resulting diblocks. It seems likely that exchange occurs

$$\text{PB–OK} + \text{LiCl} = \text{PB–OLi} + \text{KCl}$$

Since KCl is insoluble this equilibrium will lie well to the right and a proportion of the capped polydiene will be rendered inactive through self-association of the –OLi terminal moieties.

Whereas the GPC traces for the polydienes were sharp and symmetrical and corresponded to the anticipated molecular weights the traces of the diblocks gave long tails when pure THF was used as the eluting solvent. No such tails were observed when the solvent was changed to a THF/DMF mixture, showing that they were artefacts caused by adsorption on to the columns—perhaps at sites where some oxidative degradation of the column packing had occurred. The molecular weights of the PEO blocks were determined from those of the polydienes in conjunction with the composition determined from the $^1$H NMR spectra. The conversion of EO to copolymer was generally found to be complete and the polydispersities of the diblocks were in the range 1.01–1.05. Fig. 1 shows a typical example of the GPC traces of the polydiene and the diblock derived from it. $^1$H NMR showed the microstructures to be: for PI, 10% 3,4; 70% *cis*-1,4 and 20% *trans*-1,4 and for PB, 7% 1,2; 50% *cis*-1,4 and 43% *trans*-1,4.

### 3.1. SAXS from copolymers

Table 1 summarizes the compositions of the PI–PEO copolymers and the structures determined by SAXS. At ambient temperature crystalline domains of PEO are set in an amorphous matrix of PI. Above about 55 °C the crystals melt and the diblocks form lamellar microphase-separated structures—with the exception of sample YD 50 which is disordered, i.e. its $T_{ODT}$ (order–disorder transition temperature) is below the melting point of the PEO as a consequence

Table 1
Structures and domain spacings ($d$) for PI–PEO diblocks as observed by SAXS

| | $M_n$ (PI) | $M_n$ (PEO) | $N$ (PI) | $N$ (PEO) | $r_V$ (PEO) | $\phi$ (PEO) | Structure | $T_{ODT}$ | $d$ (Å) | $\chi r_V T_{max}$ |
|---|---|---|---|---|---|---|---|---|---|---|
| YD 34 | 11,000 | 13,300 | 159 | 302 | 621 | 0.49 | Lamella | >160 | 338 | 171 |
| YD 43 | 6100 | 5400 | 88 | 123 | 300 | 0.41 | Lamella | >160 | 157 | 82.4 |
| YD 41 | 4700 | 7800 | 68 | 177 | 314 | 0.57 | Lamella | >300 | 228 | 74.8 |
| YD 42 | 5800 | 18,200 | 84 | 414 | 582 | 0.71 | Lamella | >160 | 288 | 160 |
| YD 45 | 5490 | 11,660 | 80 | 265 | 424 | 0.62 | Lamella | >340 | 234 | 98.0 |
| YD 46 | 5490 | 18,670 | 80 | 424 | 584 | 0.73 | Lamella | >300 | 289 | 139 |
| YD 50 | 770 | 920 | 11 | 21 | 43 | 0.48 | Disordered | $< T_m$ (PEO) | – | 14.8[a] |

The value of $\chi r_V T_{max}$ is the value at the highest temperature reached, indicating that the ODT is above 300 °C for most of the polymers, except YD 50, where the ODT is below the melting temperature of PEO. $\phi$ (PEO) is the volume fraction of PEO.

[a] The $\chi$ value is calculated from Ref. [22].

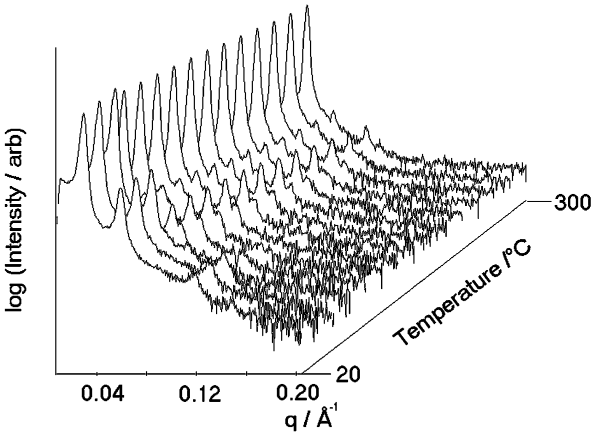

Fig. 2. Three-dimensional relief diagram of time-resolved SAXS data obtained with a time resolution of 6 s during heating and cooling of the copolymer YD 39. The heating was from 20 to 300 °C at a ramp rate of 10 °C min$^{-1}$. The plot shows $\log I(q,t)$ vs. scattering vector, $q$, vs. temperature, $T$. For clarity a limited number of slices is shown.

of the very low molecular weights of the blocks which comprise it. The three-dimensional relief plot (Fig. 2) of $\log I$ vs. the scattering vector $q$ vs. the temperature for the PB–PEO sample YD 39 typifies the morphological change ensuing from melting. The SAXS data collected for the PB–PEO blocks (Table 2) also show microphase separation above the melting point of the crystalline PEO. Hexagonal structures are observed for YD 35 and YD 39 whereas YD 37 has a lamellar structure.

To be consistent with the theory of block copolymer microphase separation, we have recast the degree of polymerization $N$, so as to take account of the different molar volumes of the constituent molecules. To do this, we have chosen the PEO monomer unit as the reference unit and converted all the degrees of polymerization into the PEO equivalent. To indicate this we use $r_V$ as opposed to $N$; $r_V$ is calculated as $r_V = m + n(V_m/V_n)$ where $m$ is the degree of polymerization of the PEO block and $V_m$ is the specific volume of the PEO block. Similarly, $n$ and $V_n$ pertain to the relevant parameters for the PI (or PB) block.

We have calculated $\chi$ based on the values given by Floudas et al. [22]. Using these values and the method described above we can determine $\chi r_V$, for our systems. These results are shown in the last column of Table 1 for the maximum temperature achieved during the SAXS run ($T_{\max}$). As can be seen from these values, we are far above the critical value of $\chi r_V$ for the ODT which, in the mean-field treatment, is of the order of 10.5. The values indicate that we are well within the strong segregation regime. This is confirmed by a power law fit to the domain spacing as a function of $r_V$, which shows an exponent of 0.66. For the strong segregation regime we would expect an exponent close to 2/3; for the weak segregation this should fall to 1/2.

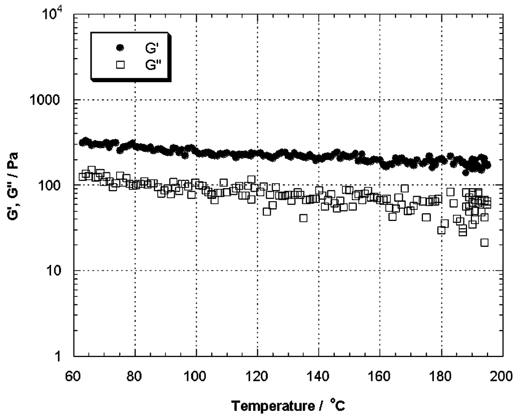

Fig. 3. Temperature dependence of the low-frequency $G'$ and $G''$ shear moduli for YD 48 Kraton L1203®–PEO diblock copolymer. 1% strain amplitude, 1 rad s$^{-1}$ frequency and 2 °C min$^{-1}$ ramp rate.

The diblock copolymers derived from Kraton L1203® (Table 3) form an interesting pair. Examination of the rheological behaviour of YD 48, which has a relatively long PEO block, shows a continuous small steady decline in the values of $G'$ and $G''$ with increasing temperature from above the melting point of the PEO to 200 °C (Fig. 3) which was reversed on cooling. This suggests that no change in morphology occurs over this range. In contrast, YD 47 which has a much shorter PEO block, shows a distinct rise in the value of $G'$ over the range of 70–80 °C (Fig. 4) suggesting the probable occurrence of a change in morphology. Further heating results in a small decrease in $G'$ until about 115 °C when it falls precipitously—clearly indicating transition to a disordered melt. On cooling $G''$ showed very pronounced hysteresis. Rather similar behaviour has been noted with some polystyrene–PI diblocks [36] which was attributed to supercooling of the high temperature morphology below the $T_{\mathrm{ODT}}$. The SAXS results (Fig. 5) show that there is an order–order transition at about 81 °C from bbc to hexagonal morphology and that there is the onset of disorder above 110 °C. Fig. 5 shows the time resolved scattering from sample YD 47; for clarity, only every 10th frame is presented. The first few frames demonstrate the semicrystalline nature of the diblock copolymer. The scattering is typified by a broad fundamental peak indicative of a wide range of fold lengths, and is

Table 2
Structure, domain spacings ($d$) and volume fraction ($\phi$) of PB–PEO diblocks. (No ODT was found for these materials below 160 °C)

| | $M_n$ (PEO) | $M_n$ (PB) | $N$ (PEO) | $N$ (PB) | $r_V$ (PEO) | $\phi$ (PEO) | $d$ (Å) | Structure |
|---|---|---|---|---|---|---|---|---|
| YD 35 | 4300 | 10,000 | 98 | 185 | 394 | 0.248 | 266 | Hexagonal |
| YD 37 | 10,600 | 4300 | 241 | 80 | 368 | 0.654 | 215 | Lamellar |
| YD 39 | 18,200 | 4500 | 414 | 83 | 547 | 0.756 | 259 | Hexagonal |

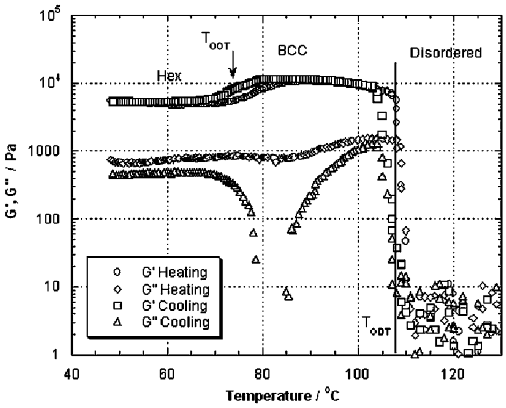

Fig. 4. Temperature dependence of $G'$ and $G''$ for YD 47 Kraton L1203-PEO® diblock copolymer during heating from 50 to 130 °C followed by cooling. Conditions: 1% strain, 5 rad $s^{-1}$ frequency and 2 °C $min^{-1}$ ramp rate.

common for 'as prepared' or solvent evaporated samples. On heating above the melting point of the PEO block, the fundamental peak from the semicrystalline PEO decreases whilst the microphase melt peak increases in intensity. It is noticeable that the peak is now sharp and well defined. Analysis shows that the structure is comprised of cylinders of the minority component PEO arranged on a two-dimensional hexagonal lattice with a characteristic domain spacing of 110 Å. On further heating, transformation to the bcc structure with a domain spacing of 103 Å occurs at about 81 °C and is now identified as the cause of the rise in the value of $G'$ observed at this temperature. Further heating results in the loss of the regular structure as the melt is transformed into a low viscosity liquid and mirrors the drastic drop in $G'$. This is the ODT, characterized by compositional fluctuations and a sharp drop in the SAXS intensity (the vertical scale is logarithmic).

Hydrogenating a PI–PB–OH diblock formed PEP–PE–OH (where PEP is poly(ethylene-*alt*-propylene) and PE is polyethylene). Conversion to the potassium salt provided a macro-initiator which was used to synthesize the triblock copolymer PEP–PE–PEO having block molecular weights of 1500, 1000 and 1850, respectively. This material is of particular interest in that it is expected to contain two different crystalline domains (PE and PEO) in a PI matrix. Wide-angle X-ray scattering confirmed this prediction and showed reflections corresponding to the overlay of those of the homopolymers but with those of the PE being somewhat broadened because the method of its synthesis led to some ethyl branches. Differential scanning calorimetry showed endotherms at about 55 °C due to the PEO and also at about 86 °C which was attributed to the melting of the PE crystals. Preliminary work on the rheology suggests an OOT at around 140 °C and an ODT around 230 °C. More extensive study is under way.

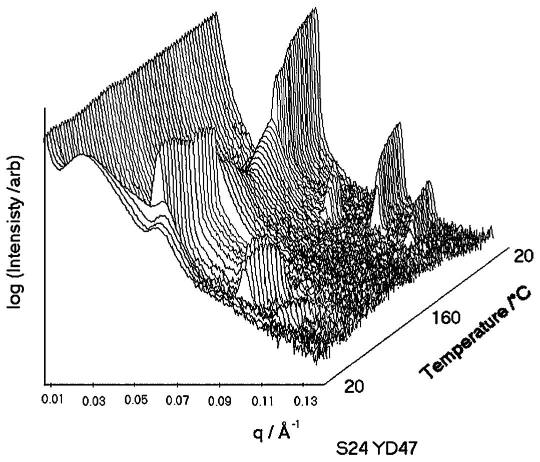

Fig. 5. Three-dimensional relief diagram of the time resolved SAXS data collected, from sample YD 47, with a time resolution of 6 s per frame and a heating rate of 10 °C $min^{-1}$. The sample was first heated to the ODT and then cooled, as indicated on the temperature scale.

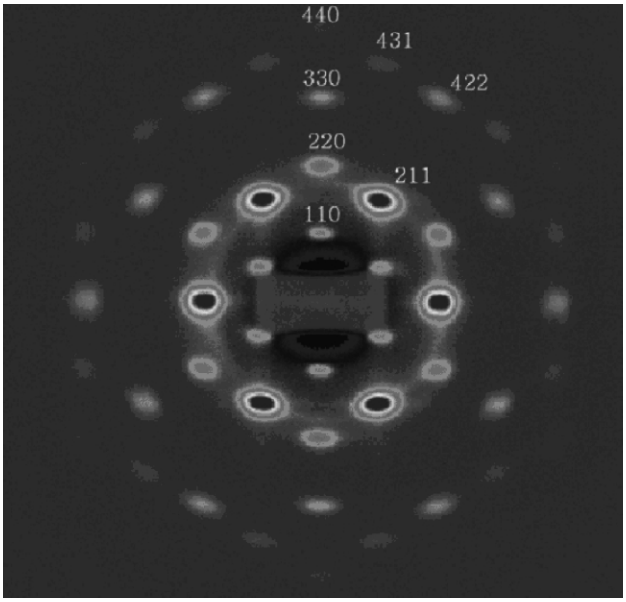

Fig. 6. SAXS pattern from YD 41 17 wt% aqueous solution. The reflections are indexed to a bcc structure; limitations of reproduction reduce the number of printed orders. The sample was hand sheared at room temperature. The domain spacing of the innermost reflection is 653 Å. (The large rectangular block is the beamstop).

### 3.2. SAXS from aqueous gels

Aqueous gel samples of YD 41 and YD 42 were investigated by SAXS. The results show strong scattering—indicative of a large X-ray contrast. This is understandable since the PB and PI blocks are much more hydrophobic than either poly(propylene oxide) (PEO–PPO) or poly(butylene oxide) (PEO–PBO) systems. Whereas the diffraction patterns of the latter two systems generally only show some 2 or 3 orders [37,38] those from YD 41 and YD 42 are very sharp and some 6 or 7 orders can be seen (Fig. 6). The room temperature, manually sheared, two-dimensional SAXS of YD 41 aqueous gel shows a bcc pattern for the 17 wt% solution in water The fundamental reflection closest

Table 3
Structures and domain spacing (*d*) of the PE/PEE–PEO diblock copolymers

| | $M_n$ (PE/PEE) | $M_n$ (PEO) | | $T_{OOT}$ (°C) | *d* (Å) | | $T_{ODT}$ (°C) | *d* (Å) |
|---|---|---|---|---|---|---|---|---|
| YD 47 | 4200 | 1140 | hex | 81 | 110 | bcc | 117 | 103 |
| YD 48 | 4200 | 8300 | – | – | – | – | >200 | – |

Table 4
Structures and domain spacings (*d*) of aqueous gel phases of YD 41 and YD 42

| Sample | Conc (wt%) | Structure | *d* (Å) |
|---|---|---|---|
| YD 41 | 17 | bcc | 653 |
| | 22 | bcc | 483 |
| | 30 | hex | 441 |
| | 35 | hex | 434 |
| | 50 | hex | 400 |
| YD 42 | 20 | bcc | 583 |
| | 30 | bcc | 529 |
| | 39 | hex | 513 |

to the beamstop is the (110) at 653 Å, giving an edge length of 462 Å for the cubic structure (Table 4). One-dimensional SAXS shows that this structure is stable up to 95 °C (the upper limit of our temperature control apparatus). On increasing the concentration of the polymer in solution to 22% the bcc pattern is retained. However, at 30% a hexagonal structure is observed, and this is also seen at 35 and 50 wt%. Thus there is a transition between the bcc and hexagonal phase between 22 and 30 wt%. We are currently investigating this further using polarized light microscopy.

A similar pattern of bcc changing to hexagonal is observed in the YD 42 sample with the 20 and 30% samples showing the bcc structure and the 39 wt% showing a hexagonal structure. Table 4 shows the observed structures and the domain spacings of the fundamental peaks. In both cases the expected decrease in domain spacing as concentration is increased is observed. This is attributable to an excluded volume effect as the overlap between micelles increases.

## 4. Conclusions

SAXS has established the morphology of six samples of PI–PEO and three of PB–PEO in the bulk state. These form micelles in water, which give up to sixth order diffraction spots. Well ordered diblocks can also be prepared from the Kraton L1203$^{\circledR}$, a commercial hydrogenated mixed-architecture polybutadiene bearing a terminal hydroxyl group. A preliminary study of a triblock copolymer PEP–PE–PEO which contains two crystallizable blocks has been made.

## References

[1] Olvera de la Cruz M, Sanchez IC. Macromolecules 1986;19:2501.
[2] Vavasour JD, Whitmore MD. Macromolecules 1993;26:7070.
[3] Fredrickson GH, Helfand E. J Chem Phys 1987;87:697.
[4] Laschewsky A. Adv Polym Sci 1955;124:1.
[5] Piirma I. Polymeric surfactants. New York: Marcel Dekker; 1992.
[6] Velichkova RS, Kristova DC. Prog Polym Sci 1995;20:819.
[7] Chiu H-C, Chern C-S, Lee H-F. Polymer 1998;39:1609.
[8] Lunsted LG. J Am Oil Chem Soc 1951;28:294.
[9] Shimura Y, Lin WS. J Polym Sci A-1 1970;8:2171.
[10] Benson RS, Wu Q, Ray AR, Lyman DJ. J Polym Sci, Polym Chem 1985;23:399.
[11] Floudas G, Tsitsilianis C. Macromolecules 1997;30:4381.
[12] Zhu L, Cheng SZD, Calhoun BH, Ge Q, Quirk RP, Thomas EL, Hsaio BS, Yeh F, Lotz B. Polymer 2001;42:5839.
[13] Xie H-Q, Tao Z-Q, Guo J-S. J Polym Sci 1996;61:407.
[14] Gervais M, Gallot B. Macromol Chem 1977;178:1577.
[15] Rahman R, Avny Y. J Macromol Sci, Chem 1979;A13:953.
[16] Hentze H-P, Kramer E, Berton B, Forster S, Antonietti M. Macromolecules 1999;32:5803.
[17] Hong S, Yang L, McKnight WJ, Gido SP. Macromolecules 2001;34:7009.
[18] Forster S, Kramer E. Macromolecules 1999;32:2783.
[19] Hirata E, Ijitsu T, Soen T, Hashimoto T, Kawai H. Polymer 1975;16:249.
[20] Allgaier J, Poppe A, Willner L, Richter D. Macromolecules 1997;30:1582.
[21] Robitaille C, Prud'homme J. Macromolecules 1983;16:665.
[22] Floudas G, Ulrich R, Wiesner U. J Chem Phys 1999;110:652.
[23] Floudas G, Vazaiou B, Schipper F, Ulrich R, Wiesner U, Iatrou H, Hadjichristidis N. Macromolecules 2001;34:2947.
[24] Hillmyer MC, Bates FS. Macromolecules 1996;29:6994.
[25] Lipic PM, Bates FS, Hillmyer MA. J Am Chem Soc 1998;120:8963.
[26] St Pierre LE, Price CC. J Am Chem Soc 1956;78:3432.
[27] Young RN, Quirk RP, Fetters LJ. Adv Polym Sci 1984;56:1.
[28] Quirk RP, Ma J-J. J Polym Sci, Polym Chem 1988;26:2031.
[29] Esswein B, Muller M. Angew Chem Int Ed Engl 1996;35:623.
[30] Forster S, Kramer E. Macromolecules 1999;32:2783.
[31] Khan TH, Mobbs RH, Price CC, Quintana JR, Stubbersfield RB. Eur Polym J 1987;23:191.
[32] Allgaier J, Poppe A, Willner L, Richter D. Macromolecules 1997;30:1582.
[33] Rachapudy H, Smith GG, Raju VR, Graessley WW. J Polym Sci 1979;17:1211.
[34] Bras W, Derbyshire GE, Ryan AJ, Mant GR, Felton A, Lewis RA, Hall CJ, Greaves GN. Nucl Instrum Meth Phys Res 1993;A326:587.
[35] Borsboom M, Bras W, Cerjak I, Detollenaere D, Glastra van Loon D, Goedtkindt P, Konijnenburg M, Lassing P, Levine YK, Munneke B, Oversluizen M, van Tol R, Vlieg E. J Synchr Rad 1998;5:518.
[36] Forster S, Khandpur AK, Zhao J, Bates FS, Hamley IW, Ryan AJ, Bras W. Macromolecules 1994;27:6922.
[37] Pople JA, Hamley IW, Fairclough JPA, Ryan AJ, Booth C, Pedersen S. Phys Macromol 1998;31:2952.
[38] Hamley IW, Pople JA, Fairclough JPA, Ryan AJ, Booth C, Yang Y-W. Macromolecules 1998;31:3906.